Available online at www.sciencedirect.com

SciVerse ScienceDirect

Ceramics International 39 (2013) 383–387

CERAMICS INTERNATIONAL

www.elsevier.com/locate/ceramint

Transparent Lu_3NbO_7 bodies prepared by reactive spark plasma sintering and their optical and mechanical properties

Liqiong An, Akihiko Ito*, Takashi Goto

Institute for Materials Research, Tohoku University, Sendai 980-8577, Japan

Received 6 June 2012; received in revised form 12 June 2012; accepted 13 June 2012
Available online 19 June 2012

Abstract

Transparent lutetium niobate (Lu_3NbO_7) bodies were prepared by reactive spark plasma sintering using Lu_2O_3 and Nb_2O_5 powders. Fully dense Lu_3NbO_7 bodies with density greater than 99.5% of the theoretical were obtained at 1300–1650 °C. The grains steadily grew from 0.1 to 0.6 μm with increasing sintering temperature from 1200 to 1450 °C and significant grain growth from 2.2 to 9.2 μm occurred at 1550–1650 °C. The Lu_3NbO_7 body sintered at 1450 °C showed the highest transmittance of 63% at 550 nm after heat treatment at 850 °C in air for 6 h. Fully dense, submicron-size transparent Lu_3NbO_7 exhibited Vickers hardness of ~13.0 GPa and indentation fracture toughness of 1.0 MPa $m^{1/2}$.

Keywords: A. Sintering; C. Optical property; D. Niobates; Transparent ceramics

1. Introduction

Rare earth niobates (RE_3NbO_7) with fluorite structure have attracted considerable interest as functional materials because of their anomalous magnetic properties and mixed ionic conductivity [1–5]. Among rare earth elements, Lu has the smallest ionic radius (97.7 pm for eight-fold coordinated Lu^{3+}) next to Sc [6], and thus Lu_3NbO_7 can preserve the $Fm\bar{3}m$ symmetry in the fluorite structure [5]. Its cubic structure is well suited for isotropic optical media. Because of the high atomic number of Lu ($Z_{Lu}=71$), Lu compounds exhibit high stopping power against high-energy beams and can be promising scintillation materials. However, no study has been conducted on the preparation of either single crystal or polycrystalline transparent Lu_3NbO_7 due to its high melting point (~2300 K) [7], whereas the heat capacity [8] and refined structural parameters [5] of Lu_3NbO_7 powder have been reported.

Spark plasma sintering (SPS) is a versatile technique for obtaining a fully dense body of a material with high melting point [9]. The short holding time and relatively low sintering temperature of SPS favour the fabrication of fine-grained, highly transparent polycrystalline bodies [10–13]. We have recently prepared a transparent Lu_3NbO_7 body by SPS using calcined powder of Lu_3NbO_7 [14]. Because there is no readily available commercial source of Lu_3NbO_7 powder, reactive sintering is the most convenient route to prepare a transparent body. However, reactive sintering has often caused insufficient reaction or subsequent grain growth during sintering, which results in opacity. Therefore, the reactive sintering process should be optimized for the preparation of a highly transparent, fully dense, fine-grained body.

In the present study, the transparent Lu_3NbO_7 bodies were prepared by reactive SPS of Lu_2O_3 and Nb_2O_5 powders. The effect of sintering and heat-treatment temperature on the microstructure, optical and mechanical properties of the Lu_3NbO_7 bodies were investigated.

2. Experimental procedure

Lu_2O_3 (Shin-Etsu Rare Earth, Tokyo, Japan; 99.99% purity) and Nb_2O_5 (Wako Pure Chemical, Tokyo, Japan; 99.9% purity) commercial powders were used as starting materials. These powders were stoichiometrically mixed (Lu:Nb=3:1) and ball milled using zirconia balls in

*Corresponding author. Tel.: +81 22 215 2106; fax: +81 22 215 2107.
E-mail address: itonium@imr.tohoku.ac.jp (A. Ito).

0272-8842/$36.00
http://dx.doi.org/10.1016/j.ceramint.2012.06.038

ethanol for 12 h. Then, the milled slurry was dried at 60 °C for 24 h and passed through a 200 mesh sieve. The obtained powder was poured into a graphite die with a diameter of 10 mm and sintered by SPS (SPS-210LX, Fuji Electric Industrial, Japan) in vacuum. Details of the sintering profile have been reported elsewhere. The sintering temperature increased from room temperature to 600 °C in 300 s and to 1200–1650 °C at 0.17 °C s^{-1}. The temperature was maintained for 5 min at 1000 °C and for 45 min at 1200–1650 °C. A pressure of 10 MPa was preloaded below 1000 °C and increased to 100 MPa above 1000 °C. The specimen was heat treated at 750–1250 °C in air for 6 h. The sintered body was mirror polished on both sides using diamond slurry (1 μm). The final thickness of the specimen was approximately 1 mm. The polished surface was thermally etched at 100–200 °C below the sintering temperature in air for 1 h to measure the grain size.

Density was measured by Archimedes method in distilled water. Phase identification was accomplished by X-ray diffraction (XRD; RAD-2C, Rigaku, Japan). The thermally etched and fracture surfaces were observed using a field emission scanning electron microscope (FE-SEM, JSM-7500F, JEOL, Japan) and a scanning electron microscope (SEM; S-3100H, Hitachi, Japan). The average grain size was determined from the linear intercept length using a statistical factor of 1.56 and counting at least 250 grains [15]. The in-line transmittance in the wavelength range of 200–800 nm was measured with a spectrophotometer (UV-3101PC, Shimadzu, Japan). Vickers hardness (H_V) and fracture toughness (K_{IC}) were measured by a hardness tester (HM-221, Mitutoyo, Japan) at room temperature. K_{IC} was calculated by the following equation, $K_{IC}=0.073P\times c^{-1.5}$, using an applied load (P) of 0.98 N and the half crack length (c) that formed at the corners of the indentation.

3. Results and discussion

Fig. 1 shows the XRD patterns of the Lu_3NbO_7 bodies sintered at 1200–1650 °C. The XRD patterns can be indexed as cubic defect fluorite Lu_3NbO_7 (space group: $Fm\bar{3}m$; $a=0.5179$ nm; ICSD# 24–6385) [5]. In the cubic-defect fluorite structure, the Lu^{3+} and Nb^{5+} cations, and O^{2-} anions statistically occupy the 4*a* and 8*c* sites, respectively. No secondary phase was observed in all specimens. The XRD peaks slightly broadened at 1200 °C (Fig. 1(a)). The peaks were sharp but with shoulders at lower angles (Fig. 1(b) and (c)). These shoulders at lower angles have often been observed in distorted defect fluorite structures, such as fully or partially stabilised ZrO_2 [16]. The Lu_3NbO_7 bodies sintered at high temperature could have the defective structure.

Fig. 2 shows the thermally etched surfaces of the Lu_3NbO_7 bodies sintered at 1200–1650 °C. Pores were observed in the Lu_3NbO_7 body sintered at 1200 °C (Fig. 2(a)) and the specimen became fully dense having a uniform microstructure at 1400 and 1450 °C (Fig. 2(b) and (c)). Significant grain growth was observed at 1650 °C (Fig. 2(d)). Fig. 3 shows the fracture surfaces of the Lu_3NbO_7 bodies sintered at 1200–1550 °C. A porous and not well-sintered microstructure was observed at 1200 °C (Fig. 3(a)). At 1400–1450 °C, pores were rarely observed, and the fracture mode was mainly transgranular (Fig. 3(b)–(d)). The fracture mode became intergranular at 1550 °C (Fig. 3(d)).

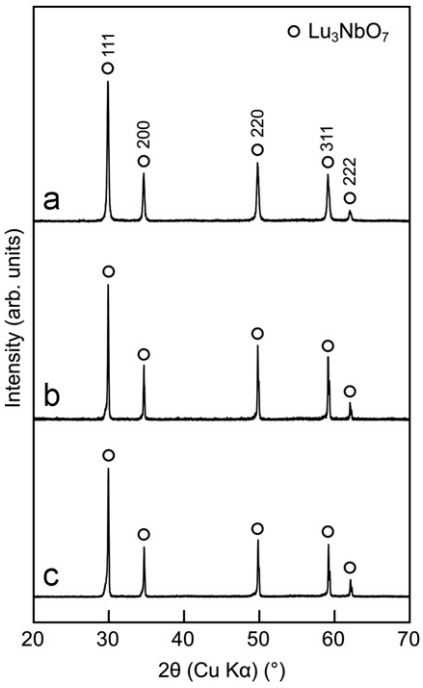

Fig. 1. XRD patterns of Lu_3NbO_7 bodies sintered at various temperatures: 1200 °C (a), 1450 °C (b) and 1650 °C (c).

Fig. 4 shows the effect of sintering temperature on the relative density and average grain size of the Lu_3NbO_7 bodies. The relative density was 81.7% of the theoretical density at 1200 °C, which agrees with the porous microstructure (Fig. 3(a). Fully dense Lu_3NbO_7 (greater than 99.5% of the theoretical density) was obtained at 1300–1650 °C. The grain size steadily increased from 0.1 to 0.6 μm with increasing sintering temperature from 1200 to 1450 °C. Significant grain growth occurred at 1650 °C, and the average grain size reached 9.2 μm.

The as-sintered body had a black colour due to the reducing atmosphere during SPS. Fig. 5 displays optical micrographs of Lu_3NbO_7 bodies sintered at 1450 °C after heat treating at 750–1250 °C in air for 6 h. At 800 °C, the Lu_3NbO_7 body had a black part inside the specimen (Fig. 5(a)). The heat-treated Lu_3NbO_7 body at 850 °C became transparent and colourless (Fig. 5(b)). The Lu_3NbO_7 bodies were transparent but partially frosted at 950 °C and 1050 °C (Fig. 5(c) and (d)).

Fig. 6 shows the effect of the heat-treatment temperature on the transmittance spectra of the Lu_3NbO_7 bodies sintered at 1450 °C. The transmittance was low at the heat treatment temperature of 750 °C because the colour remained after the heat treatment (curve a in Fig. 6). At heat-treatment

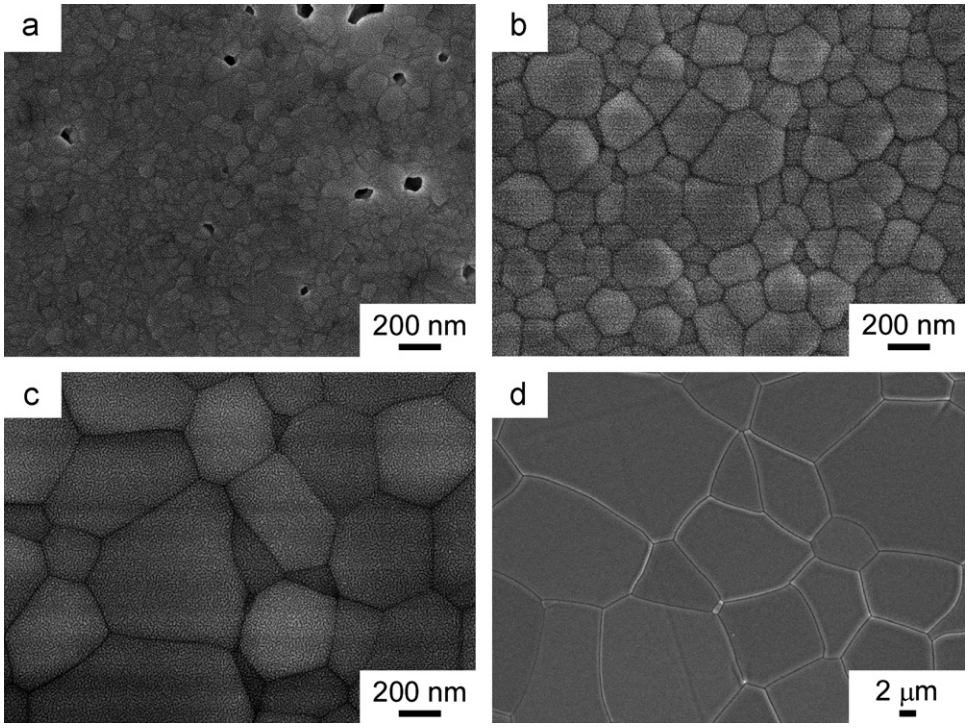

Fig. 2. Thermally etched surfaces of Lu_3NbO_7 bodies sintered at various temperatures: 1200 °C (a), 1400 °C (b), 1450 °C (c) and 1650 °C (d).

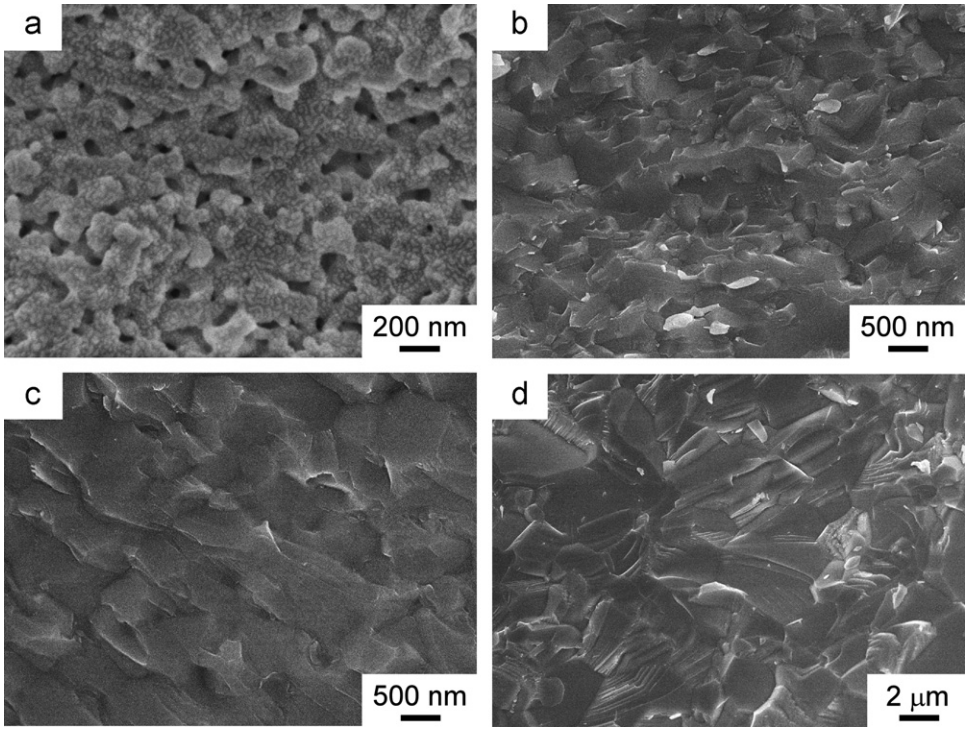

Fig. 3. Fracture surfaces of Lu_3NbO_7 bodies sintered at various temperatures: 1200 °C (a), 1400 °C (b), 1450 °C (c) and 1550 °C (d).

temperatures of 850–1050 °C, the colour disappeared and transmittance increased significantly (curve b in Fig. 6). With further increase in the heat-treatment temperature, transmittance in the ultraviolet range increased slightly (curves c and d in Fig. 6). The transmittance declined at 1150 °C (curve e in Fig. 6). At 1250 °C, the sintered body was milky white (curve f in Fig. 6). A similar behaviour has been observed in ZrO_2 [17] and $Lu_2Ti_2O_7$ [18] because of the increase in pore sizes

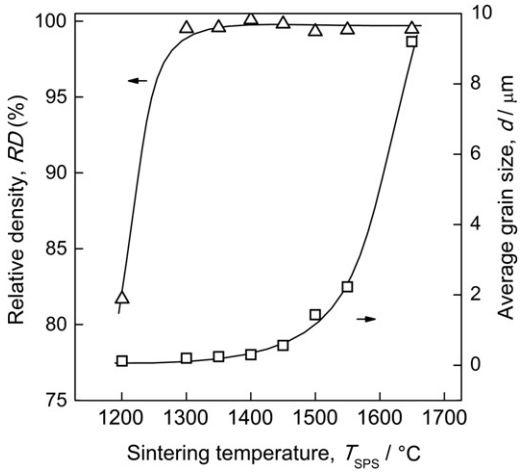

Fig. 4. Effect of sintering temperature on relative density and average grain size of Lu_3NbO_7 bodies.

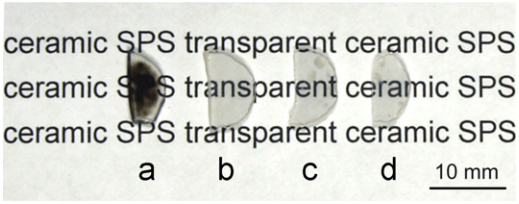

Fig. 5. Optical photographs for Lu_3NbO_7 bodies sintered at 1500 °C and heat-treated at various temperatures in air for 6 h: 750 °C (a), 850 °C (b), 950 °C (c) and 1050 °C (d).

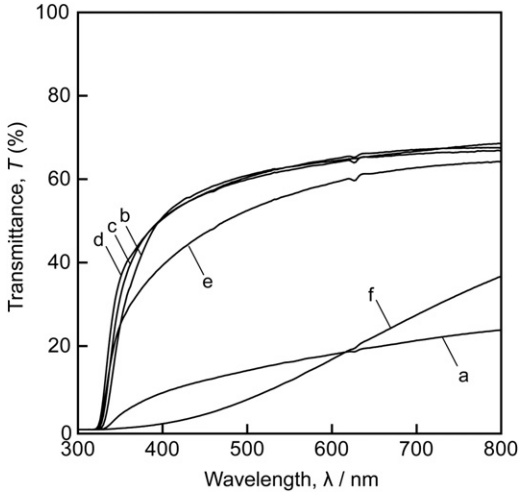

Fig. 6. Transmittance of Lu_3NbO_7 bodies sintered at 1450 °C and heat-treated at various temperatures in air for 6 h: 750 °C (a), 850 °C (b), 950 °C (c), 1050 °C (d), 1150 °C (e) and 1250 °C (f).

and grain growth during the high-temperature heat treatment. The black colour of the as-sintered bodies disappeared after heat treatment at 850–1050 °C in air.

Fig. 7 shows the transmittance spectra of the Lu_3NbO_7 bodies sintered at 1300–1550 °C after heat treatment at 850 °C in air for 6 h. The transmittance increased with sintering temperature (curves a–d in Fig. 7), exhibiting a

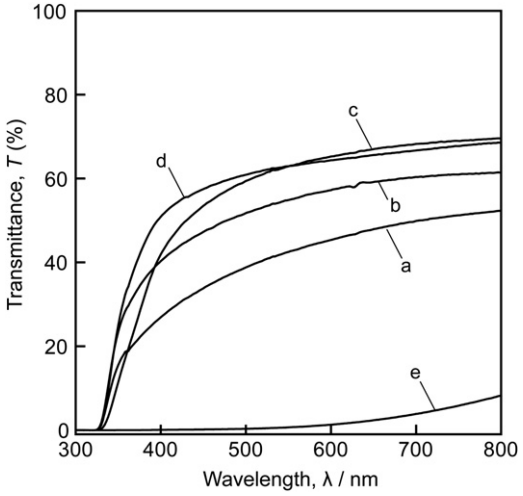

Fig. 7. Transmittance of of Lu_3NbO_7 bodies sintered at various temperatures: 1300 °C (a), 1400 °C (b), 1450 °C (c), 1500 °C (d) and 1550 °C (e). Heat treatment at 850 °C in air for 6 h.

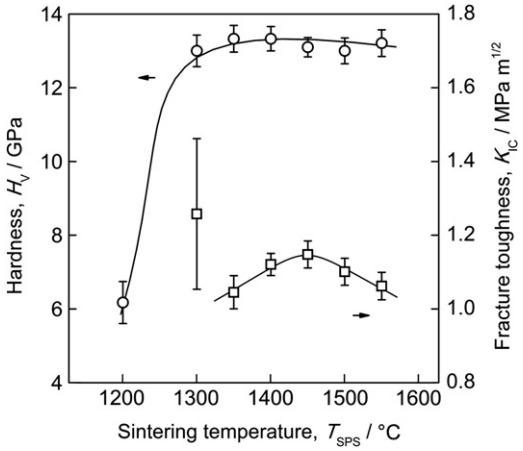

Fig. 8. Effect of sintering temperature on Vickers hardness and indentation fracture toughness of Lu_3NbO_7 bodies after heat treatment at 850 °C in air for 6 h.

maximum of 63% at 550 nm at 1450 °C (curve d in Fig. 7). This value is comparable to that of 68% at 550 nm for the transparent Lu_3NbO_7 body, prepared by SPS using calcined Lu_3NbO_7 powder [14]. The transmittance decreased at 1550 °C (curve e in Fig. 7). The low and high sintering temperatures resulted in sintered bodies with porous structure and grain coarsening, respectively, thereby degrading transmittance. The optimal sintering temperature was 1450 °C due to high relative density (99.8%) and submicron grains (0.6 μm).

Fig. 8 shows the effect of sintering temperature on the Vickers hardness (H_V) and the indentation fracture toughness (K_{IC}) of the Lu_3NbO_7 bodies after heat treatment. The Lu_3NbO_7 body sintered at 1200 °C had a low H_V of 6.2 GPa due to the low relative density of 81.7%. H_V increased to 13 GPa at 1300 °C and ranged from 13.0 to 13.3 GPa at 1350–1550 °C. K_{IC} ranged between 1.0–1.1 MPa m$^{1/2}$ for the SPS temperatures of 1350–1550 °C.

4. Conclusions

Transparent Lu_3NbO_7 bodies were prepared by SPS. Single-phase Lu_3NbO_7 bodies were obtained at sintering temperatures of 1200–1650 °C. A fully dense Lu_3NbO_7 body with density above 99.5% of the theoretical value was obtained at 1300–1650 °C. Low and high sintering temperatures (below 1400 °C and above 1550 °C) resulted in porous structures and grain coarsening, respectively, thereby degrading transmittance. The optimal sintering temperature was 1450 °C due to the high relative density (99.8%) and submicron grains, leading to the highest transmittance of 63% at 550 nm after heat treatment at 850 °C in air for 6 h.

Acknowledgments

This research was supported in part by the Research Fellowships of the Japan Society for the Promotion of Science for Young Scientists. This research was also supported in part by the Global COE Program of Materials Integration, Tohoku University, and in part by the Grant-in-Aid for Challenging Exploratory Research (#24655186), MEXT, Japan.

References

[1] J.G. Allpress, H.J. Rossell, Fluorite-related phases Ln_3MO_7, Ln=rare earth, Y, or Sc, M=Nb, Sb, or Ta. I. Crystal chemistry, Journal of Solid State Chemistry 27 (1979) 105–114.

[2] M.P. van Dijk, K.J. de Vries, A.J. Burggraaf, Oxygen ion and mixed conductivity in compounds with the fluorite and pyrochlore structure, Solid State Ionics 9–10 (1983) 913–919.

[3] M. Wakeshima, Y. Hinatsu, Magnetic properties and structural transitions of orthorhombic fluorite-related compounds Ln_3MO_7 (Ln=rare earths, M=transition metals), Journal of Solid State Chemistry 183 (2010) 2681–2688.

[4] L. Cai, J.C. Nino, Structure and dielectric properties of Ln_3NbO_7 (Ln=Nd, Gd, Dy, Er, Yb and Y), Journal of the European Ceramic Society 27 (2007) 3971–3976.

[5] Y. Doi, Y. Harada, Y. Hinatsu, Crystal structures and magnetic properties of fluorite-related oxides Ln_3NbO_7 (Ln=lanthanides), Journal of Solid State Chemistry 182 (2009) 709–715.

[6] R.D. Shannon, Revised effective ionic radii and systematic studies of interatomic distances in halides and chalcogenides, Acta Crystallographica Section A 32 (1976) 751–767.

[7] T.G. Babich, A.V. Zagorodnyuk, G.A. Teterin, L.V. Sadkovskaya, A.P. Zhirnova, System Y_2O_3-Nb_2O_5. Binary phase equilibria, Soviet Progress in Chemistry 55 (1989) 21–24.

[8] A.N. Klimenko, Y.S. Kozlov, V.S. Sergeev, E.A. Pastukhov, High temperature phase transitions in rare-earth element niobates R_3NbO_7, Thermochimica Acta 209 (1992) 331–338.

[9] Z.A. Munir, U. Anselmi-Tamburini, M. Ohyanagi, The effect of electric field and pressure on the synthesis and consolidation of materials: a review of the spark plasma sintering method, Journal of Materials Science 41 (2006) 763–777.

[10] B.-N. Kim, K. Hiraga, K. Morita, H. Yoshida, T. Miyazaki, Y. Kagawa, Microstructure and optical properties of transparent alumina, Acta Materialia 57 (2009) 1319–1326.

[11] R. Chaim, R. Marder, C. Estournès, Optically transparent ceramics by spark plasma sintering of oxide nanoparticles, Scripta Materialia 63 (2010) 211–214.

[12] L.Q. An, A. Ito, T. Goto, Effects of ball milling and post-annealing on the transparency of spark plasma sintered Lu_2O_3, Ceramics International 37 (2011) 2263–2267.

[13] L.Q. An, A. Ito, T. Goto, Highly transparent lutetium titanium oxide produced by spark plasma sintering, Journal of the European Ceramic Society 31 (2011) 237–240.

[14] L.Q. An, A. Ito, T. Goto, Fabrication of transparent Lu_3NbO_7 by spark plasma sintering, Materials Letters 65 (2011) 3167–3169.

[15] M.I. Mendelson, Average grain size in polycrystalline ceramics, Journal of the American Ceramic Society 52 (1969) 443–446.

[16] J. Kondoh, Origin of the hump on the left shoulder of the X-ray diffraction peaks observed in Y_2O_3-fully and partially stabilized ZrO_2, Journal of Alloys and Compounds 375 (2004) 270–282.

[17] U. Anselmi–Tamburini, J.N. Woolman, Z.A. Munir, Transparent Nanometric Cubic and Tetragonal Zirconia obtained by high-pressure pulsed electric current sintering, Advanced Functional Materials 17 (2007) 3267–3273.

[18] L.Q. An, A. Ito, T. Goto, Effects of sintering and annealing temperature on fabrication of transparent $Lu_2Ti_2O_7$ by spark plasma sintering, Journal of the American Ceramic Society 94 (2011) 3851–3855.